

Osmotic instabilities in active membrane tubes

Sami C. Al-Izzi,^{1,2} George Rowlands,² Pierre Sens,³ and Matthew S. Turner^{2,4}

¹Department of Mathematics, University of Warwick, Coventry CV4 7AL, UK

²Department of Physics, University of Warwick, Coventry CV4 7AL, UK

³CNRS, Physicochimie Curie - UMR 168, Institut Curie,

11 rue Pierre et Marie Curie, 75231 Paris cedex 05, France

⁴Centre for Complexity Science, University of Warwick, Coventry CV4 7AL, UK

We study a membrane tube with unidirectional ion pumps driving an osmotic pressure difference. A pressure driven peristaltic instability is identified, quantitatively distinct from similar tension-driven Rayleigh type instabilities on membrane tubes. We discuss how this instability could be related to the function and biogenesis of membrane bound organelles, in particular the contractile vacuole complex. The unusually long natural wavelength of this instability is in close agreement with that observed in cells.

Self-organisation and self-assembly are prevalent throughout the biological world. Although the “blueprint” for internal cellular structures is genetically encoded, the cell must ultimately rely on physical methods of organization to build its internal structures. A key contemporary challenge in cellular biophysics is to understand the physical self-organization and regulation of organelles [1, 2]. Most models of the shape regulation of membrane bound organelles invoke local driving forces through membrane proteins altering the morphology (often curvature) [3, 4]. However other mechanisms, such as osmotic pressure, could play an important role [5].

Eukaryotic organelles bound by lipid membranes perform a variety of mechanical, electrical and chemical functions inside the cell, and range in size, construction, and complexity [6]. A quantitative understanding of how such membrane bound organelles function could have applications in bioengineering, synthetic biology and medicine.

Membrane tubes are found in many organelles such as the Golgi and endoplasmic reticulum [6]. Models for their formation typically involve the spontaneous curvature of membrane proteins [4] or forces arising from molecular motors, attached to the membrane, that pull tubular tethers as they move along microtubules [7]. Many of these tubules contain trans-membrane proteins which can alter the osmotic pressure by active transport of ions. Most work on the biogenesis of cellular organelles has focused on their static morphology and generally not on their non-equilibrium dynamics. In what follows we consider an example in which the out of equilibrium dynamics can be shown to drive the morphology. Our study is motivated by the biophysics of an organelle called the Contractile Vacuole Complex.

The Contractile Vacuole Complex (CVC) is an organelle found in most freshwater protists and algae that regulates osmotic pressure by expelling excess water [9–12]. There are many different classifications of CVC’s depending upon the exact structure of the organelle, which vary between species [8]. A large amount of electrophysiology data and imaging has been collected for the CVC in *Paramecium multimicronucleatum* [10, 13–16],

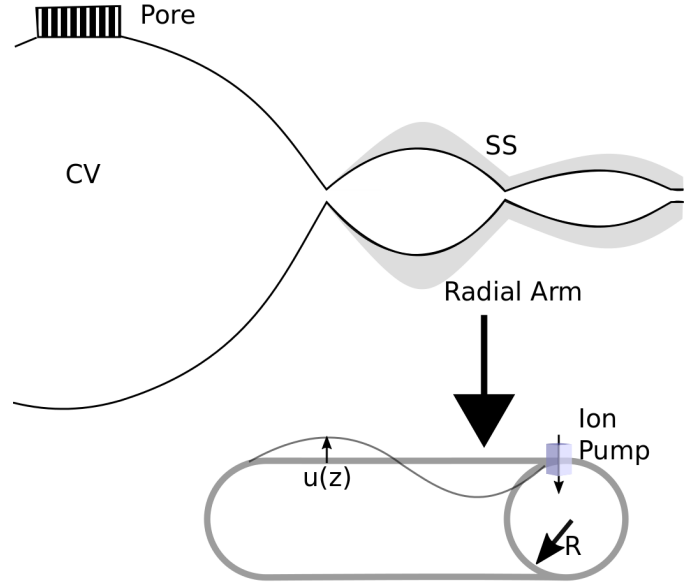


FIG. 1. Sketch of the morphology of the CVC in *Paramecium multimicronucleatum* showing the main vesicle (CV) anchored to the plasma membrane pore. The radial arm is surrounded by the smooth spongiome (SS), and contains unidirectional ion pumps. A more detailed diagram can be found in [8]

see FIG. 1. Our analysis is motivated by CVC’s of this form that contain a main vesicle, known as the Contractile Vacuole (CV), which is anchored to the cell membrane by a pore. Attached to the main vesicle are 5 – 10 membrane tubes (radial arms). Surrounding these tubes is a membrane structure resembling a bicontinuous phase, called the smooth spongiome (SS). The membrane tubes are inflated due to water influx due to an osmotic gradient. This gradient is generated by Adenosine Triphosphate (ATP)-hydrolysing proton pumps in the membrane that moves protons into the CV, causing it to become hypertonic to the cytosol [10, 17–19]. After the CV reaches some threshold, the pore attaching it to the cell membrane opens, allowing water to be expelled. The whole cycle then repeats with a period that depends on the ionic concentration of the external medium/cytosol but

that is typically 20 – 30s [11]. Evidence from images of the CV taken during the final “rounding phase” of the main vesicle, just before solvent expulsion, show that the tubes swell and later re-inflate the CV after it has emptied [14].

The radial arms of the CV appear to be undergoing a process similar to the Pearling or Rayleigh instability of a tube under high tension [20–24] or Axons under osmotic shock [25], but with a longer natural wavelength (Rayleigh instabilities have a natural wave length $\lambda \sim R$ where R is the tube radius). Inspired by this similarity we attempt to understand the morphology and initial growth phase of the radial arms by looking for instabilities in the physical equations describing the fluid and membrane. We treat the smooth spongione as a reservoir of membrane at constant tension everywhere along the tube. While this is certainly an approximation it seems to be a reasonable starting point and also allows us to make substantial analytic progress.

The CVC is comprised of a phospholipid bilayer membrane. This bilayer behaves in an elastic manner [26, 27]. At physiological temperatures the lipids that make it up are in the fluid phase [6, 27]. It is also known that the two monolayer “leaflets” of the bilayer can follow different dynamics, exerting shear stresses on each other [28–30]. For simplicity we will treat the bilayer as a purely elastic, fluid membrane in the constant tension regime, neglecting the separate dynamics of each leaflet.

We shall assume a homogeneous lipid membrane, that does not change topology, so that the Helfrich model of the membrane as an elastic differentiable manifold provides a reasonable approximation to the membrane energy [26, 31, 32].

This manifold has mean curvature H and constant surface tension γ . The smooth spongione is identified as a putative membrane reservoir and, for simplicity, we assume that this maintains constant membrane tension everywhere. The free energy for such a membrane is

$$\mathcal{F} = \int_{\mathcal{S}} dA \left(\frac{\kappa}{2} (2H)^2 + \gamma \right), \quad (1)$$

where dA is the area element on \mathcal{S} and κ is the bending rigidity. The pressure difference between the fluid inside and outside the tube, P , leads to an additional contribution to the energy of the form $-\int P dV$. Assuming radial symmetry and integrating over the volume of the tube we obtain

$$\mathcal{F} = 2\pi \int_{-\infty}^{\infty} \frac{\kappa}{2} r \frac{1}{\sqrt{1 + (\partial_z r)^2}} \left(\frac{\partial_{zz} r}{1 + (\partial_z r)^2} - \frac{1}{r} \right)^2 + \gamma r \sqrt{1 + (\partial_z r)^2} - \frac{1}{2} r^2 P dz \quad (2)$$

where z and $r(z, t)$ are the usual cylindrical coordinates, see S.I. for details.

We will use Eq. (2) as a model for the free energy of a radial arm of the CVC. Instabilities are driven by an

expansion in volume due to an osmotic pressure difference caused by ion pumps in the surface of the tube. In this section we set up a model of such a system and calculate the dominant modes of the instability in the limit where the tube length is much longer than the equilibrium radius. Ion Pumps cause a flux of water to permeate through the membrane. We write the radius of the tube as $r(z, t) = R + u(z, t)$, with u assumed small, and make use of the Fourier representation $u(z, t) = \sum_q \bar{u}_q e^{iqz}$. Absorbing the $q = 0$ mode into $R = R(t)$, we can write $\int u dz = 0$.

Hence the free-energy per unit length can be written at leading order as

$$\mathcal{F} = \mathcal{F}^{(0)} + \frac{\pi}{R} \sum_q \alpha(q) |\bar{u}_q|^2 \quad (3)$$

where

$$\alpha(q) = \frac{\kappa}{R^2} \left(Q^4 - \frac{Q^2}{2} + 1 \right) + \gamma Q^2 - PR \quad (4)$$

with $Q = qR$ and

$$\mathcal{F}^{(0)} = 2\pi \left(\frac{\kappa}{2R} + \gamma R - \frac{1}{2} PR^2 \right) \quad (5)$$

By computing the Laplace pressure in terms of γ and R , ($PR = -\kappa/(2R^2) + \gamma$), the point at which the $q = 0$ mode goes unstable can be identified: the membrane tube is unstable for tube radii $R > \sqrt{3}R_{eq}$ where $R_{eq} = \sqrt{\frac{\kappa}{2\gamma}}$ is the equilibrium radius of a tube with $P = 0$. This criterion for the *onset* of the instability is the same as the Rayleigh instability on a membrane tube [23], however the instability is now driven by pressure not surface tension. In what follows we are interested in the dynamics of the growth of unstable modes after the cylinder has reached radius $\sqrt{3}R_{eq}$.

We consider the initial growth phase of the arm starting from a tube with no net pressure at $t = 0$. This is a model of the development of the instability. After the instability is fully developed the CVC empties and the process repeats. Proton pumps in the membrane move ions from the cytosol into the radial arm of the CV. We denote the number of ions per unit length in the tube as n and assume that the number of ion pumps depends only on the initial surface area, i.e. it is fixed as the volume (and surface) increases/decreases. We can then write an equation for the growth of n as

$$\frac{dn}{dt} = \begin{cases} 0, & t \in (-\infty, 0) \\ 2\pi\beta R_{eq}, & t \in [0, \infty) \end{cases} \quad (6)$$

where β is a constant equal to the pumping rate of a single ion pump multiplied by the area density of ion pumps.

The density of ions, ρ_I , can be obtained by solving Eq. (6) and dividing by volume per unit length, $v(t)$,

$$\rho_I = \frac{n(t)}{v(t)} = \frac{n_0}{v(t)} + \frac{2\pi\beta R_{eq}t}{v(t)}. \quad (7)$$

The growth of the tube radius is driven by a difference between osmotic and Laplace pressure [33]. This means the rate equation for the increase in volume per unit length, $v(t)$, can be written in terms of the membrane permeability to water $\mu' = \mu a$, where μ is the permeability per unit area per unit length, a . Thus

$$\frac{dv}{dt} = \mu' (k_B T (\rho_I - \rho_I(t=0)) - P) \quad (8)$$

where the osmotic pressure is approximated by an ideal gas law.

Assuming that the number of water permeable pores is constant, we can write an equation for $R(t)$ on the time interval $t \in [0, \infty)$. We identify P with the Laplace pressure. This leads to

$$\frac{d\tilde{R}}{d\tilde{t}} = \frac{\tau_{\text{pump}}}{\tau_\mu} \frac{1}{\tilde{R}} \left(\frac{\tilde{t}}{\tilde{R}^2} + \left(1 + \frac{\tilde{\gamma}}{\tilde{R}} \right) \left(\frac{1}{\tilde{R}^2} - 1 \right) \right) \quad (9)$$

where $\tilde{\gamma} = \frac{\gamma}{k_B T R_{eq} \rho_I(t=0)}$, $\tau_{\text{pump}} = \frac{R_{eq} \rho_I(t=0)}{2\beta}$, $\tilde{t} = \frac{t}{\tau_{\text{pump}}}$, $\tilde{R} = \frac{R}{R_{eq}}$ and $\tau_\mu = \frac{R_{eq}}{\mu k_B T \rho_I(t=0)}$. τ_{pump} and τ_μ can be thought of as the time-scales of pumping and permeation of water respectively. These dynamics assume our ensemble conserves surface tension, not volume (consistent to the Rayleigh instability). This proves to be a crucial difference.

An estimate for permeability $\mu = 10^{-4} \mu\text{m Pa}^{-1}\text{s}^{-1}$ of polyunsaturated lipid membranes is available in the literature [34], although this value would depend heavily on concentration of water channels. Values of $R_{eq} = 25\text{nm}$, $\gamma = 10^{-4}\text{N m}^{-1}$ and hence κ are estimated using experimentally measured values from [35, 36]. We take a typical ionic concentration in the cytosol of a protist for $\rho_I(t=0) = 3.0 \times 10^8 \mu\text{m}^{-3}$ (around 10 mMol) [10, 27, 37]. Making an order of magnitude estimate of β from the literature on the CVC [10, 15, 16] leads to estimates of $\beta \approx \tilde{\beta} \times 2 \times 10^6 \mu\text{m}^{-2}\text{s}^{-1}$ where $\tilde{\beta} \in [1, 10^3]$. Temperature is taken as $T = 310\text{K}$. $\tau_\mu / \tau_{\text{pump}} \sim \tilde{\beta} \times 10^{-3}$, hence allowing a multiple time-scales expansion [38] of Eq. (9), with $\tilde{\gamma} \sim 10^{-4}$ we find the approximate asymptotic solution

$$\tilde{R}(t) = \left(\frac{t}{\tau_{\text{pump}}} + 1 \right)^{1/2} + \mathcal{O} \left(\frac{\tau_\mu}{\tau_{\text{pump}}} \right) \quad (10)$$

where $1/\tau_{\text{pump}} = \frac{2\beta}{\rho(t=0)R_{eq}} = 0.5546\tilde{\beta} \text{ s}^{-1}$. This solution agrees well with numerical solutions to Eq. (9). Using Eq. (10) and Eq. (4) we can compute the time at which each q mode goes unstable, see S.I.

We now proceed to deriving the dynamical equations for the Fourier modes. The equations governing the bulk flow are just the standard inertia free fluid equations for velocity field \vec{v} . These are the continuity equation for incompressible flow

$$\vec{\nabla} \cdot \vec{v} = 0 \quad (11)$$

and the Stokes equation

$$\vec{\nabla} P = \eta \nabla^2 \vec{v} \quad (12)$$

where P is the pressure and $\eta = 10^{-3}\text{Pa} \cdot \text{s}$ the viscosity. The system has the following linearised boundary conditions

$$v_r|_{r=R} = \dot{u} \quad (13)$$

$$v_z|_{r=R} = 0 \quad (14)$$

the second condition is justified by invoking the membrane reservoir as a mechanism for area exchange.

Solving these equations and substituting into the force balance equation at the membrane gives

$$\dot{\bar{u}}_q = -\frac{\alpha(q)q^2 R(t)}{8\eta} \bar{u}_q \quad (15)$$

where \bar{u}_q is the Fourier representation of u in the z direction, for more details on this derivation see S.I. and [23]. The dispersion relation is now time dependant, hence instead of looking at the maximum, we solve for the growth of all the modes, see S.I. for more details.

The fluctuations of modes with wavenumber q about the radius $R(t)$ follow the dynamics of the Langevin equation based on Eq. (15)

$$\eta(q)\dot{\bar{u}}_q = -\alpha(q)\bar{u}_q + \zeta_q \quad (16)$$

where $\eta(q) = \frac{8\eta}{Rq^2}$ and ζ_q , the thermal noise, has the following statistical properties

$$\langle \zeta_q \rangle = 0 \quad (17)$$

$$\langle \zeta_q(t_1) \zeta_{q'}(t_2) \rangle = \delta_{qq'} \delta(t_1 - t_2) \frac{k_B T R \eta(q)}{\pi}. \quad (18)$$

Here the thermal noise is found using the equipartition theorem, and is thus integrated around the radius of the tube.

Using this to solve the equation for $\langle |\bar{u}_q|^2 \rangle$, following the switching-on of the ion pumps at $t = 0$, we find

$$\begin{aligned} \langle |\bar{u}_q|^2 \rangle &= \langle |\bar{u}_q|^2(0) \rangle \exp \left(-2 \int_0^t \frac{\alpha(q)}{\eta(q)} dt' \right) \\ &+ \int_0^t \frac{2k_B T R}{2\pi\eta(q)} \exp \left(-2 \int_{t'}^t \frac{\alpha(q)}{\eta(q)} dt'' \right) dt' \end{aligned} \quad (19)$$

where t'' is a time variable integrating over the noise kernel.

Assuming that the tube has had an infinite time to equilibrate before the pumps switch on, $\langle |\bar{u}_q|^2(0) \rangle$ can be found by the equipartition theorem.

Using the approximate solution for $\tilde{R}(t)$ we can calculate an exact integral formula for $\langle |\bar{u}_q|^2 \rangle$, see S.I. for more details. Integrating this numerically we can find the dynamics of the modes, where varying $\tilde{\beta}$ has the effect of changing the time-scale on which the modes go unstable.

The distribution of mode amplitude against q is shown in FIG. 2. Although the smallest q modes go unstable first, they have a very low growth rate and so the mode that dominates the instability involves a balance between

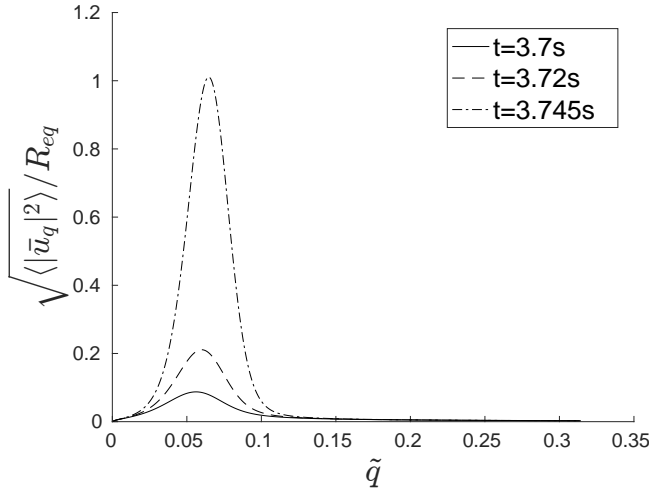


FIG. 2. Plot of the distribution of mode amplitude $\sqrt{\langle \bar{u}_q^2 \rangle}$ against scaled wavenumber $\tilde{q} = qR_{eq}$ for $t = 3.7$ s (solid), 3.72 s (dashed) and 3.745 s (dash-dotted, the time when the first modes are $\sqrt{\langle \bar{u}_q^2 \rangle} = R_{eq}$), $\tilde{\beta} = 1$.

going unstable early (favouring low q) and growing fast (favouring high q).

We can compute the natural wavelength associated with the first mode to reach $\sqrt{\langle \bar{u}_q^2 \rangle} = R_{eq}$ as we vary β , FIG. 3, and find that the natural wavelength $\lambda \sim 1\mu\text{m}$ across the entire range of values of physiological β . The natural wavelength appears to have a slower than logarithmic dependence on the pumping rate β , with faster pumping favouring only slightly shorter wavelength modes. The lack of dependence of the dominant wavelength (to linear order) of the instability on the pumping rate is due to the fact that an increase in $\tilde{\beta}$ also increases the growth rate of the unstable modes (as well as making them unstable earlier). Hence a large change in $\tilde{\beta}$ changes the dominant wavelength only marginally, although the time-scale of the instability is now much shorter. The difference in dominant wavelength from a Rayleigh instability is partially due to the increase in radius causing an increase in the magnitude of the q^4 term in $\alpha(q)$, Eq. (4), which stabilizes higher \tilde{q} modes. The dominant wavelength is different from that realised under an osmotic shock in the same ensemble. This is due to the quasi-static pumping of the system giving lower \tilde{q} modes more time to grow, see S.I. for details. It is a combination of both of these factors which produces this new long wavelength morphology.

This wavelength is of the right order of magnitude observed in the CVC ($\lambda \sim 1 - 5\mu\text{m}$ [11]). It is also a quantitatively different instability to the Rayleigh or Perling instability where $\lambda \sim R_{eq}$ [21, 22, 24] as its natural wavelength is about two orders of magnitude larger than the tube radius. It is fortuitous that this frequency does not depend heavily on $\tilde{\beta}$, the parameter we can estimate least accurately. The experimental time-scale of the radial arm

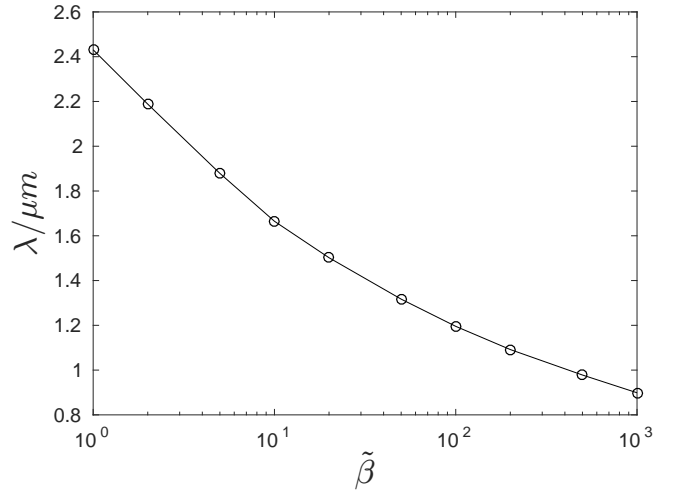


FIG. 3. Plot of natural wavelength of the pressure driven instability on the membrane tube λ in micrometers against $\tilde{\beta}$, the parameter controlling pumping rate.

inflation, found from optical microscopy imaging, is consistent with a value of $\tilde{\beta} \sim 1 - 10$ or $\tau_{\text{pump}} \sim 1 - 10^{-1}\text{s}$.

To conclude, we have analysed a simple model of a leaky membrane tube containing uni-directional active ion pumps. Deriving dynamical equations for the tube modes we are able to identify an instability that is driven by osmotic imbalance and then to compute its wavelength. This instability has a natural frequency that is found to be $\lambda \sim 1\mu\text{m}$, significantly different from a Rayleigh or Perling instability, and close to the instability length scale observed on the CVC radial arm. We speculate that this instability may provide a mechanism for biogenesis of the CV from a featureless active tube: The instability generates bulges in the radial arm that are also of a size that is comparable to the main CV. This will be the subject of future work.

Thanks to J. Prost and P. Bassereau (Paris), M. Polin (Warwick) and R. G. Morris (Bangalore) for interesting discussions and insight. S. C. Al-Izzi would like to acknowledge funding supporting this work from EPSRC under grant number EP/L015374/1, CDT in Mathematics for Real-World Systems.

-
- [1] C. Mullins, *The Biogenesis of Cellular Organelles*, 1st ed. (Springer, 2005).
 - [2] Y.-H. M. Chan and W. F. Marshall, *Science* **337**, 1186 (2012).
 - [3] R. Heald and O. Cohen-Fix, *Current Opinion in Cell Biology* **26**, 79 (2014), cell architecture.
 - [4] Y. Shibata, J. Hu, M. M. Kozlov, and T. A. Rapoport, *Annual Review of Cell and Developmental Biology* **25**, 329 (2009).
 - [5] D. Gonzalez-Rodriguez, S. Sart, A. Babataheri, D. Tareste, A. I. Barakat, C. Clanet, and J. Husson,

- Phys. Rev. Lett. **115**, 088102 (2015).
- [6] B. Alberts, A. Jihson, J. Lewis, M. Raff, K. Roberts, and P. Walter, *Molecular Biology of The Cell*, 5th ed. (Garland Science, 2008).
 - [7] A. Yamada, A. Mamane, J. Lee-Tin-Wah, A. D. Cicco, D. Levey, J.-F. Joanny, E. Coudrier, and P. Bassereau, *Nature communications* **5**, 3624 (2014).
 - [8] D. J. Patterson, *Biological Reviews* **55**, 1 (1980).
 - [9] K. Komsic-Buchmann, L. Wöstehoff, and B. Becker, *Eukaryotic Cell* **13**, 1421 (2014).
 - [10] C. Stock, H. K. Grønlien, R. D. Allen, and Y. Naitoh, *Journal of cell science* **115**, 2339 (2002).
 - [11] R. D. Allen, *BioEssays* **22**, 1035 (2000).
 - [12] Y. Naitoh, T. Tominaga, M. Ishida, A. K. Fok, M. Aihara, and R. D. Allen, *The Journal of experimental biology* **200**, 713 (1997).
 - [13] T. Tominaga, R. Allen, and Y. Naitoh, *The Journal of experimental biology* **201**, 451 (1998).
 - [14] T. Tominaga, Y. Naitoh, and R. D. Allen, *Journal of cell science* **112** (Pt **2**, 3733 (1999).
 - [15] R. D. Allen and A. K. Fok, *J. Protozool* **35**, 63 (1988).
 - [16] T. Tani, R. Allen, and Y. Naitoh, *J. Exp. Biol.* **203**, 239 (2000).
 - [17] J. Heuser, Q. Zhu, and M. Clarke, *Journal of Cell Biology* **121**, 1311 (1993).
 - [18] T. Nishi and M. Forgac, *Nature Reviews Molecular Cell Biology* **3**, 94 (2002).
 - [19] A. K. Fok, M. S. Aihara, M. Ishida, K. V. Nolta, T. L. Steck, and R. D. Allen, *Journal of cell science* **108** (Pt **1**, 3163 (1995).
 - [20] T. R. Powers and R. E. Goldstein, *Physical Review Letters* **78**, 2555 (1997).
 - [21] R. Bar-Ziv and E. Moses, *Physical Review Letters* **73**, 1392 (1994).
 - [22] R. Bar-Ziv, T. Tlusty, and E. Moses, *Physical Review Letters* **79**, 1158 (1997).
 - [23] K. L. Gurin, V. V. Lebedev, and A. R. Muratov, *Journal of Experimental and Theoretical Physics* **83**, 321 (1996).
 - [24] P. Nelson, T. Powers, and U. Seifert, *Physical Review Letters* **74**, 3384 (1995).
 - [25] P. A. Pullarkat, P. Dommersnes, P. Fernández, J. F. Joanny, and A. Ott, *Physical Review Letters* **96**, 1 (2006).
 - [26] W. Helfrich, *Zeitschrift für Naturforschung C* **28**, 693 (1973).
 - [27] R. Phillips, J. Kondev, J. Theriot, and H. Garcia, *Physical Biology of The Cell*, 2nd ed. (Garland Science, 2012).
 - [28] U. Seifert and S. A. Langer, *Europhysics Letters (EPL)* **23**, 71 (1993).
 - [29] E. Evans and A. Yeung, *Chemistry and Physics of Lipids* **73**, 39 (1994).
 - [30] J. B. Fournier, *International Journal of Non-Linear Mechanics* **75**, 67 (2015).
 - [31] S. A. Safran, *Statistical Thermodynamics of Surfaces, Interfaces, and Membranes*, 1st ed. (Westview Press, 2003).
 - [32] D. Nelson, T. Piran, S. Weinberg, M. E. Fisher, S. Leibler, D. Andelman, Y. Kantor, F. David, D. Bertrand, L. Radzihovsky, M. J. Bowick, D. Kroll, and G. Gompper, *Statistical Mechanics of Membranes and Surfaces*, 2nd ed. (World Scientific, 2008).
 - [33] M. Chabanon, J. C. Ho, B. Liedberg, A. N. Parikh, and P. Rangamani, *Biophysical Journal* **112**, 1682 (2017).
 - [34] K. Olbrich, W. Rawicz, D. Needham, and E. Evans, *Biophysical Journal* **79**, 321 (2016).
 - [35] J. Zimmerberg and M. M. Kozlov, *Nature reviews. Molecular cell biology* **7**, 9 (2006).
 - [36] G. Koster, M. VanDuijn, B. Hof, and M. Dogterom, *Proceedings of the National Academy of Sciences of the United States of America* **100**, 15583 (2003).
 - [37] M. B. Jackson, *Molecular and Cellular Biophysics*, 1st ed. (Cambridge University Press, 2006).
 - [38] J. D. Murray, *Asymptotic Analysis*, 1st ed. (Springer, 1984).